JMEPEG (2012) 21:2691–2694
DOI: 10.1007/s11665-012-0393-y

1059-9495/$19.00

Investigation on Mechanical Properties of Deformation TiNi Thin Films

Y.H. Li, M.K. Li, F.L. Meng, and W.T. Zheng

(Submitted March 15, 2012; in revised form September 6, 2012)

The TiNi thin films were deposited onto copper substrates by magnetron sputtering. Tensile tests were carried out on CSS-44100 electron universal test-machine. X-ray diffraction profile Fourier analysis method and the Nano-Hardness Tester have been used to study the mechanical properties of deformation TiNi thin films. The mechanical properties of metals and alloys should be determined primarily by dislocation structure among these objects. The results showed that the dislocation density and the deformation storage energy density increased with the increasing elongation. Microhardness was calculated from the dislocation data. The results showed that the microhardness values were not having good agreement when comparing the calculated values with the measured values. The oxide layer on the surface and the precipitated phases of TiNi thin film affect the measured values of microhardness. The microhardness measured values were larger than the calculated values. The surface micrographs of the TiNi thin film were obtained using scanning electron microscopy (SEM). The experimental results showed that a series of parallel cracks grew in a concerted fashion across the thin film, and the cracks were equally spaced.

Keywords deformation storage energy density, microhardness, TiNi alloy, x-ray diffraction profile analysis

1. Introduction

Recently, shape memory alloys (SMAs) have attracted great attention, and their properties have been extensively studied to meet the increased demands for micro-actuators (Ref 1-3). TiNi SMA thin film shows the characteristics of large recovery stress and strain, high corrosion resistance, and high work density. It is a perfect micro-actuator candidate for the micro-electrical mechanical system (MEMS), which require actuation and sensing mechanisms with high efficiency, insofar as the mechanical properties of films are concerned (Ref 4-7). Tensile tests have been reported elsewhere (Ref 8, 9), but the deformations reported in those articles are only related to the study of stress-induced martensitic transformation. So far, no study relating to the dislocation density and the Vickers microhardness values to the strain in the film has been reported. The microhardness values of coating materials can be obtained mainly from indentation, which is a well-known and reliable method. However, the measured value of hardness is influenced by the substrate materials and the surface oxidation. According to the definition of the material's hardness, it is plausible to relate the hardness of a material to the plastic flow stress. Therefore, the hardness can be deduced directly from the crystal defects. Wang and co-workers (Ref 10) first adopted the x-ray diffraction profile analysis method to evaluate the hardness of coatings directly from the dislocation density and dislocation distribution parameter. In the present study, using the same methods, we have investigated the change of the dislocation density and the Vickers microhardness values during tension.

2. Experimental

The NiTi thin films were deposited onto Cu substrates by magnetron sputtering. The copper substrates were pre-punched into dog-bone specimens with 4.5 mm × 30 mm (gauge portion) × 35 μm (thickness). The sputtering conditions were as follows: argon pressure, 4×10^{-2} Pa; sputtering power, 640 W; deposition rate, 95 nm/min; and substrate-to-target distance, 65 mm. The substrate temperature was about 673 K. The thickness of the NiTi film was about 20 μm. The film's composition determined by energy dispersive x-ray spectroscopy was about Ti-51.45at.%Ni. The as-deposited films were first solution treated at 1073 K for 1 h, and then aged at 773 K for 30 min in a vacuum furnace. Tensile tests were carried out on CSS-44100 electron universal testing machine at ambient temperature. The strain rate was 2.2×10^{-4} s^{-1}. The stress-strain curve of the free-standing film was obtained from the experimental curve of copper substrate together with the thin film adhesive to the substrate compared with the curve of copper substrate without film. X-ray diffraction was carried out using a Rigaku 12 kW rotating and a graphite monochromator. The average crack spacing of the NiTi thin film was measured

This article is an invited paper selected from presentations at the International Conference on Shape Memory and Superelastic Technologies 2011, held November 6-9, 2011, in Hong Kong, China, and has been expanded from the original presentation.

Y.H. Li, College of Sciences, Harbin Engineering University, 145 Nantong Street, Harbin 150001, China; **M.K. Li**, State Key Lab Superhard Materials, Jilin University, Changchun 130012, China; and **F.L. Meng** and **W.T. Zheng**, Department of Materials Science, Key Laboratory of Automobile Materials of MOE, Jilin University, Changchun 130012, China. Contact e-mails: yonghuali@hrbeu.edu.cn and mfl@jlu.edu.cn.

using scanning electron microscopy (SEM). The mechanical properties were studied by MTS IIXP Nano-Hardness Tester, with a three-sided pyramidal Berkovich diamond indenter. In this study, the max penetration depth was 1000 nm, and the indentation was done at six different regions of the films to avoid errors.

3. Results and Discussion

3.1 Theory

We let $h(x)$ be the measured profile of (hkl) diffraction of the sample, and $g(x)$ the measured profile from a standard annealed sample as the instrument broadening profile. The physical broadening profile $f(x)$ can be obtained by Fourier deconvolution method given by Stokes (Ref 11):

$$h(x) = \int_{-\infty}^{\infty} f(x)g(x-y)dy. \quad \text{(Eq 1)}$$

Each profile was divided into 60 parts for calculating the Fourier transform coefficients. In the physical broadening profile:

$$f(x) = \sum_n \left(A_n \frac{\cos 2\pi nx}{60} + B_n \frac{\sin 2\pi nx}{60} \right). \quad \text{(Eq 2)}$$

As B_n is much smaller than A_n, it may be neglected, while A_n is normalized to $A_0 = 1$. It should be pointed out that $A_n = A(L)$, were $L = lt$, $t = 0, 1, 2, 3, \ldots$, l is the reflection order. According to the Warren-Averbach method (Ref 12), assuming

$$A_l(L) = A_l^s(L) * A^p(L), \quad \text{(Eq 3)}$$

where $A_l(L)$ is the Fourier coefficient of the diffraction profile; $A_l^s(L)$ and $A^p(L)$ are the strain broadening and the size broadening coefficients, respectively, and l is the reflection order, with $A^p(L)$ being independent of l. There is only one strong diffraction profile which can be precisely measured. Based on the theory (Ref 13, 14), we have the following relations:

$$A(L) = A^p(L)\, A^s(L), \quad \text{(Eq 4)}$$

$$A^p(L) = \alpha - \frac{L}{D}, \quad \text{(Eq 5)}$$

$$A^s(L) = \exp[-2\beta_c L - \pi(\beta_g)^2 L^2], \quad \text{(Eq 6)}$$

where α is the hook coefficient, D is the coherent domain size, β_c and β_g are the integral widths of Cauchy and Gaussian functions, respectively. From a series of $A^p(L)$ values for a single profile, one can obtain α, D, β_c, and β_g using the least-squares fitting procedure. Finally, the apparent dislocation density ρ^* and the apparent dislocation distribution parameter M^* can be deduced. According to the model of dislocation configuration, $k = \beta_c/(\sqrt{\pi}\beta_g)$ being the relative value of dislocations arranged in dipoles (ρ_d) and in pile-ups (ρ_p). All dislocations can be divided into two parts specified by ρ_d and ρ_p, the dislocation densities in dipoles and pile-ups, respectively. Therefore,

$$\beta_c \propto \sqrt{\rho_d},\ \beta_g \propto \sqrt{\rho_p} \quad \text{(Eq 7)}$$

In order to find the average dislocation density ρ and the average dislocation distribution parameter M in terms of the measured β_c and β_g, one must establish the dependence of the root mean square strain $\langle \varepsilon^2 \rangle^{1/2}$ on ρ and M. Wang and co-workers (Ref 13) ingeniously utilized first a set of experimental curves to determine the characteristic values ρ^* and M^* on the basis of Wilkens' study for single crystals (Ref 15). The average ρ and M are obtained using a formula. The formula depends on the diffraction vector $g(hkl)$ and Poisson's ratio υ for a particular structure.

Wang and co-workers (Ref 16) introduced a conception called the average elastic stored energy per unit volume, $\left\langle \frac{E}{V} \right\rangle$ (J/m^3). $\left\langle \frac{E}{V} \right\rangle$ is regarded as the internal average microstress and may be calculated by a formula:

$$\left\langle \frac{E}{V} \right\rangle = AGb^2 \rho \ln \frac{2M}{b\sqrt{\rho}}, \quad \text{(Eq 8)}$$

where b is the Burger's vector. G is the shear modulus, $A = 1/4\pi$ for screw dislocation, $A = 1/[4\pi(1-\upsilon)]$ for edge dislocation, and υ is Poisson's ratio.

The characterization of material properties is carried out when the materials have different intrinsic microscopic objects, such as electron structure, atom distribution, point defect constituents, dislocation configuration, etc., by macro, micro, and mesoscopic approaches (Ref 17). The mechanical properties of metals and alloys should be determined primarily by dislocation structure among these objects. The Vickers hardness values are

$$H_V\ (\text{MPa}) = \frac{10^{n+1} Gb[M(\rho)^{1/2} + (bd)^{-1/2} + 0.08^{1/2}/D]}{3.27 \times 8\pi(1-\upsilon)}, \quad \text{(Eq 9)}$$

where d is the grain size, D is the subgrain size, and n ($n < 1$) is the index of work hardening.

3.2 Results and Discussion

The strong diffraction line profiles from NiTi (110) and (220) austenite phase are recorded, respectively, and are shown

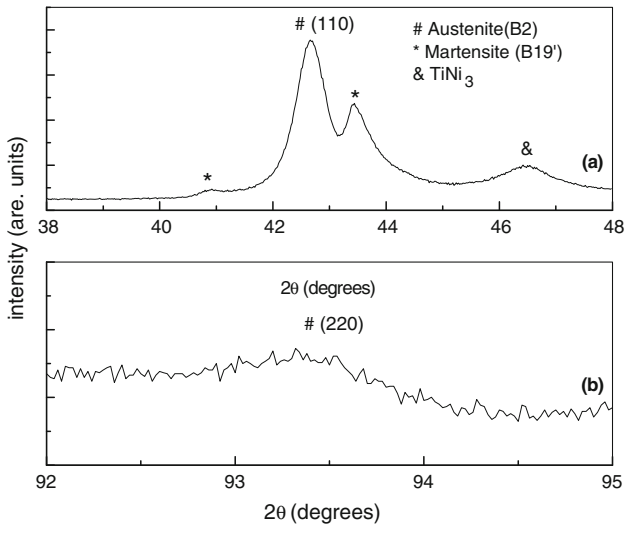

Fig. 1 The x-ray diffraction line profile of NiTi thin film (a) (110) and (b) (220) planes (austenite phase)

Table 1 Dislocation structure parameters and the calculated values of NiTi thin films

Strain, %	D, nm	ρ^*, 10^{11} cm^{-2}	M^*	ρ^*, 10^{11} cm^{-2}	M	$\left\langle \frac{E}{V} \right\rangle$, 10^6 J/m^3	Calculated values H_V, MPa	Measured values H_V, MPa
0	41.0	1.424	1.052	3.875	1.030	3.780	239.8	2547
1.4	36.9	3.019	2.333	8.211	2.284	8.653	509.6	2923
2.3	33.1	6.487	2.735	17.742	6.350	20.957	711.1	4052
3.5	32.8	7.656	3.251	20.824	7.495	24.955	2154.1	4872

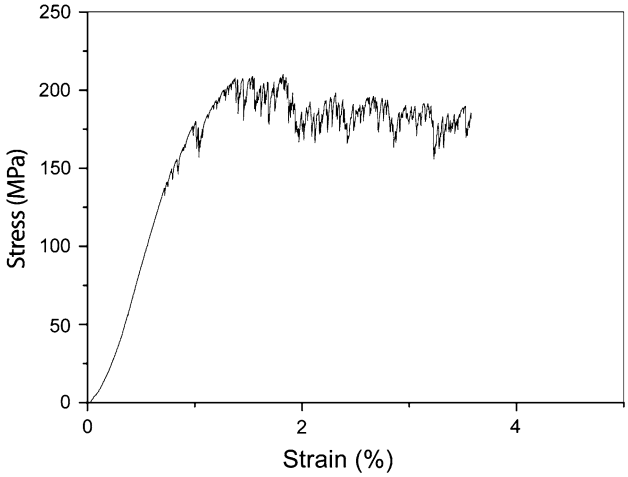

Fig. 2 The stress-strain curves of NiTi thin film

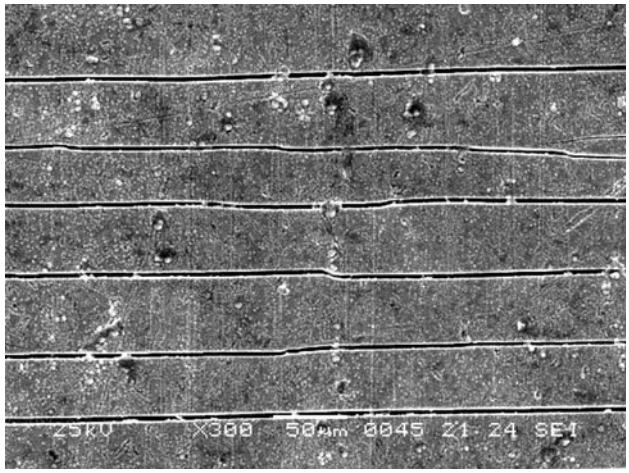

Fig. 3 The SEM micrographs of NiTi thin film

in Fig. 1. The dislocation density and the dislocation distribution parameter in thin films are deduced with x-ray diffraction profile analysis method. $\left\langle \frac{E}{V} \right\rangle$ and H_V can be determined from Eq 8 and 9, respectively. For NiTi alloy, $n = 0.2$, $\upsilon = 0.28$, $G = 2.7 \times 10^4$ MPa, $b = 0.2596$ nm (Ref 18). The grain size is estimated to be 1.2 μm from the microstructures of the thin film after heat treatment (Ref 19). The dislocation parameters and the calculated values $\left\langle \frac{E}{V} \right\rangle$ and H_V are listed in Table 1.

Figure 2 shows the stress-strain curve of NiTi thin film. The stress-strain curve can be divided into two stages. The first linear stage corresponds to the elastic deformation of the parent phase (Ref 20). In the following stage, serrations are observed.

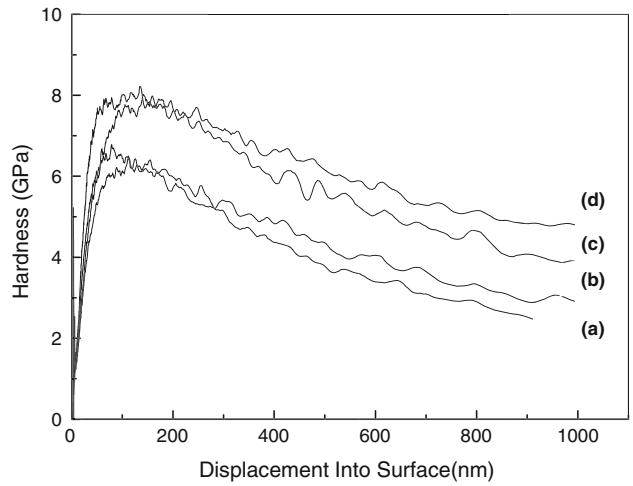

Fig. 4 Indentation hardness of TiNi thin film as a function of displacement into surface at different elongation (a) $\varepsilon = 0$; (b) $\varepsilon = 1.4\%$; (c) $\varepsilon = 2.3\%$; (d) $\varepsilon = 3.5\%$

The serrations are considered to be the stress relaxation due to the cracks propagation and precipitation. From Table 1, the average dislocation density and the average elastic stored energy density values gradually increase as strain increases. Figure 3 shows the SEM micrographs of NiTi thin film. In Fig. 3, a series of cracks grow parallel to one another, and the direction of crack extension is perpendicular to the one of tension and the cracks are about equally spaced.

During tension, the average dislocation density of NiTi thin film increases with the increasing elongation. Frank and Read (Ref 21) discussed a possible explanation for this phenomenon in terms of the reflection and multiplication of dislocation. The hardness of materials is its resistance to local plastic deformation. The average elastic stored energy density $\left\langle \frac{E}{V} \right\rangle$ is increased with increase in elongation, and the Vickers hardness calculated values also increase. From Table 1, we obtain that the Vickers hardness measured values are larger than the calculated values. This difference is caused by the oxide layer on the surface of NiTi thin film. After heat treatment in a vacuum furnace, the samples are covered by an oxide layer with thickness of a few nanometers (Ref 22). The intrinsic hardness of the film can be gained by x-ray diffraction line profile analysis from information of dislocation.

Figure 4 shows the indentation hardness of TiNi film versus the displacement into surface. The maximal hardness of annealed films appears at the surface of films. The hardness of the sample is between 6 and 8 GPa. When the distance into surface exceeded 1000 nm the hardness of all the samples becomes gradually stable. We propose the reason of this phenomenon is that a layer of TiO_2 forms on the surface of TiNi

thin film. Leng (Ref 23) investigated the hardness of TiO_2 was 19 GPa, some factors might influence the hardness of TiO_2 films, such as defects, compact degree and so on.

4. Conclusions

The mechanical properties of sputtering-deposited Ti-51.45at.% Ni thin film are investigated. The experimental results show that a series of parallel cracks grew in a concerted fashion across the thin film, and the cracks are about equally spaced. The average dislocation density and the average elastic stored energy density values gradually increase as strain increases. The Vickers hardness calculated values also increase. The indentation hardness values are larger than the calculated values. The oxide layer on the surface and the precipitated phases of NiTi thin film affect the measured values of microhardness.

Acknowledgments

This study forms part of the projects supported by the Harbin Engineering University, China (Grant No. HEUFT08035), and the Fundamental Research Funds for the Central Universities.

References

1. Y.Q. Fu, H. Du, W. Huang, S. Zhang, and M. Hu, TiNi-Based Thin Films in MEMS Applications: A Review, *Sensors Actuators A*, 2004, **112**, p 395–408
2. Y.Q. Fu, W. Huang, H. Du, X. Huang, J. Tan, and X. Gao, Characterization of TiNi Shape-Memory Alloy Thin Films for MEMS Applications, *Surf. Coat. Technol.*, 2001, **145**, p 107–112
3. B. Winzek, S. Schmitz, H. Rumpf, T. Sterzl, R. Hassdorf, S. Thienhaus, J. Feydt, M. Moske, and E. Quandt, Recent Developments in Shape Memory Thin Film Technology, *Mater Sci Eng. A*, 2004, **378**, p 40–46
4. A.K. Nanda Kumar, M.D. Kannan, and S. Jayakumar, Investigations on the Mechanical Behaviour of Rough Surfaces of TiNi Thin Films by Nano Indentation Studies, *Surf. Coat. Technol.*, 2006, **201**, p 3253–3259
5. A. Kumar, S.K. Sharma, and S. Bysakh, Effect of Substrate and Annealing Temperatures on Mechanical Properties of Ti-Rich NiTi Films, *J. Mater. Sci. Technol.*, 2010, **26**(11), p 961–966
6. A.K.N. Kumar, C.K.S. Nair, and M.D. Kannan, TEM and Nanoindentation Studies on Sputtered Ti40Ni60 Thin Films, *Mater. Chem. Phys.*, 2006, **97**, p 308–314
7. L.B. Tong, Y.H. Li, and F.L. Meng, Investigation on Mechanical Properties of Sputtered TiNi Thin Films, *J. Alloys Compd.*, 2010, **494**, p 166–168
8. S.G. Malhotra, Z.U. Rek, S.M. Yalisove, and J.C. Bilello, Analysis of Thin Film Stress Measurement Techniques, *Thin Solid Films*, 1997, **301**, p 45–54
9. B. Gabry, C. Lexcellent, V.H. No, and S. Miyazaki, Thermodynamic Modeling of the Recovery Strains of Sputter-Deposited Shape Memory Alloys Ti-Ni and Ti-Ni-Cu Thin Films, *Thin Solid Films*, 2000, **372**, p 118–133
10. N. Zhang and Y. Wang, Dislocations and Hardness of Hard Coatings, *Thin Solid Films*, 1992, **214**, p 4–5
11. A.R. Stokes, A Numerical Fourier-Analysis Method for the Correction of Widths and Shapes of Lines on X-ray Powder Photographs, *Proc. Phys. Soc. Lond.*, 1948, **61**, p 382–391
12. B.E. Warren, *Progress in Metal Physics*, vol. 8, Pergamon, London, 1959, p 147
13. Y. Wang, S. Lee, and Y. Lee, X-Ray Line Profile Analysis of Deformed Al, *J. Appl. Crystallogr.*, 1982, **15**, p 35–38
14. W. Yuming and Z. Ziqung, X-Ray Line Profile Analysis of Dislocations and Stacking Faults in Deformed Copper, *Appl. Phys. A*, 1984, **35**, p 109–114
15. M. Wilkens, *Phys. Status Solidi A*, 1970, **2**, p 359–370
16. F. Teng and Y. Wang, X-Ray Analysis of Microscopic Structure in Deformed Brass, *J. Mater. Sci.*, 1986, **21**, p 3223
17. E. Kotomin, M. Zaiser, and W. Soppe, A Mesoscopic Approach to Radiation-Induced Defect Aggregation in Alkali Halides Stimulated by the Elastic Interaction of Mobile Frenkel Defects, *Philos. Mag.*, 1994, **70**, p 317
18. F. Shan, Y. Huo, F. Teng, and Y. Wang, Dislocation and Phase Transformation in Thin Films of the Shape Memory Alloy TiNi, *Rare Met. Mater. Eng.*, 1998, **27**, p 199–201
19. F. Meng, Y. Li, Y. Wang, and W. Zheng, The Flow Stress of Ni-Rich NiTi Thin Film, *J. Mater. Sci.*, 2005, **40**, p 537–538
20. A. Ishida, M. Sato, T. Kimura, and S. Miyazaki, Stress-Strain Curves of Sputter-Deposited Ti-Ni Thin Films, *Philos. Mag. A*, 2000, **80**, p 967–980
21. F.C. Frank and W.T. Read, Multiplication Processes for Slow Moving Dislocation, *Phys. Rev.*, 1950, **79**, p 722–723
22. Y.H. Li, L.M. Li, F.L. Meng, and W.T. Zheng, Effect of Substrate Temperature on the Surface and Interface Oxidation of NiTi Thin Films, *J. Electron Spectrosc. Relat Phenom.*, 2006, **151**, p 144
23. Y.X. Leng, Structure and Properties of Ti-O-N Films, *Surf. Coat. Technol.*, 2002, **156**, p 295–300